Bulletin T.CXLVI de l'Académie serbe des sciences et des arts – 2014
Classe des Sciences mathématiques et naturelles
Sciences mathématiques, № 39

NONLINEAR DYNAMICS OF CELLULAR MICROTUBULES

MILJKO SATARIĆ

(Presented at the 7th Meeting, held on October 29, 2010)

A b s t r a c t. Microtubules are cylindrically shaped cytoskeletal biopolymers that are essential for cell motility, cell-division and intracellular trafficking by motor proteins kinesin and dynein.

In neuronal cells they play the important roles in higher cognitive functions including learning, memory and consciousness. Experimental evidence suggests that microtubules act as biological electrical wires that can transmit and amplify electric signals via the flow of condensed ionic clouds.

We here present some of our contributions aimed to elucidate the versatile biological functions in microtubules.

The used abbreviations: microtubule (MT)*, tubulin tail* (TT)*, electric elementary unit* (EEU)*.*

AMS Mathematics Subject Classification (2000): 92C05, 92C10.

Key Words: Microtubule; living cell; nonlinear dynamics; liquid crystal; polyelectrolyte; transmission line.

1. *Introduction*

Microtubules (MTs) are protein filaments of the cytoskeleton and are found in nearly all eukaryotic cells as almost the most abundant proteins [1].

MTs are typical soft-matter objects which possess high regularity and cylindrical symmetry. Their softness is brought about by the fact that the forces which underlie the polymer formation and maintain its structure are primary weak hydrogen bonds and van der Waals forces while much stronger covalent forces are responsible for creation of primary molecular structures, ie the formation of constituent amino acids and polypeptide chains.

The covalent bonds are with typical binding energy of $(2-6)\,eV$ per single bond. The hydrogen bond involves sharing of a hydrogen atom between the interacting partners in a way that H atom is covalently bonded to one partner and weakly attached to the other one by its excess charge. The representative example for biopolymers is the bond of this kind

$$-O-H\ \cdots\ N- \quad ,$$

where symbol $-$ stands for covalent bond and $\cdots$ represents corresponding hydrogen bond. The strength of hydrogen bond amounts approximately $0.2\,eV$.

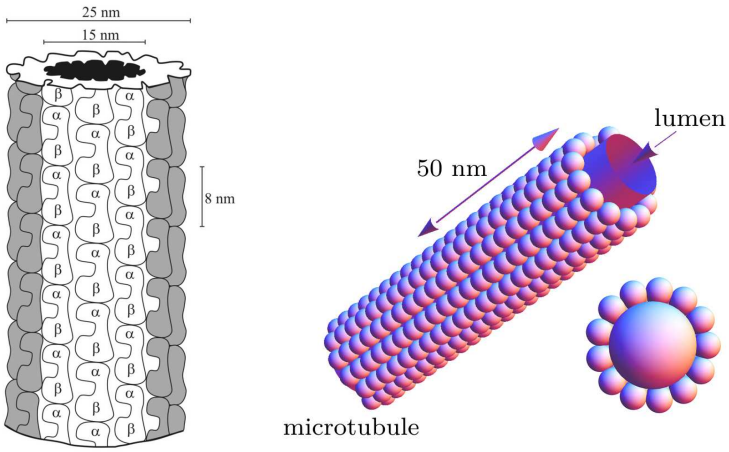

Fig. 1. (left) A MT hollow cylinder of 13 parallel protofilaments with denoted characteristic dimensions: outer and inner diameters of 25 nm and 15 nm, respectively, and tubulin dimer length of 8 nm; (right) Microtubules cross section with 13 protofilaments

The van der Waals interaction arises from mutual electric polarization of constituent molecules. It is relatively the weakest one and is of the magnitude of $(0.01-0.02)\,eV$ which is comparable with thermal energy of $0.025\,eV$.

MTs are very dynamic polymers whose assembly and disassembly is determined by whether their constituents called tubulin dimers are in a straight or tilted conformation. The cylindrical polymer of a MT has its largest diameter of roughly $25\,nm$ and a hollow lumen with a diameter of roughly $15\,nm$, see Fig. 1.a.

The lengths of MTs span dimensions from the order of micrometers to the order of millimeters. These hollow cylinders are formed by linear rows of joint heterodimers called protofilaments aligned in directions that are parallel to MT axes.

There are in vivo usually 13 longitudinally ordered protofilaments covering the walls of MTs, Fig. 1.b.

MTs form an important part of cellular scaffold which maintains the shape and stability of the cell. They also provide a network of "rails" for active intracellular transport by kinesin and dynein motor proteins [2,3]. They play a crucial role during cell division forming a dynamic structure that spatially separates duplicated chromosomes.

The building block of a MT is a tubulin heterodimer (TD) that contains approximately 900 amino acid residues comprising some 14000 atoms with a combined mass of $110\,kDa$ ($1\,Da$ is the atomic unit of mass, $1\,Da = 1.67 \cdot 10^{-27}\,kg$). Each heterodimer within a MT is effectively an electric dipole with α and β tubulin being as positive and negative side of dipole, respectively, see (Fig. 2.a).

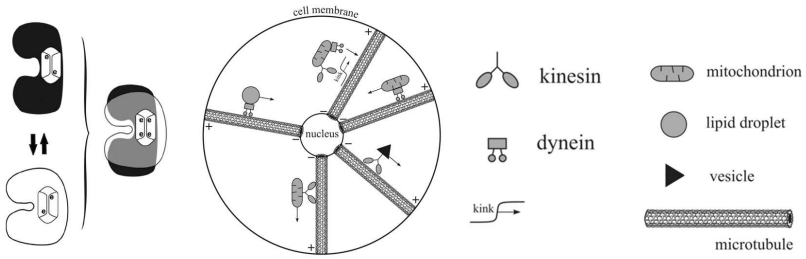

Fig. 2. (left) Dipolar moments of tubulin heterodimers; (right) The radial distribution of microtubules within a cell; The motor proteins are shown in cellular traffic

The relevant dimensions are the dimer length $\ell = 8\,nm$ and the dipolar charges displacement $d = 4\,nm$. In that respect MT is also electrically polar representing the giant dipole as the superposition of all equally oriented

heterodimers in 13 protofilaments. MTs are always oriented with positively charged ends towards a cell nucleus and the oppositely charged ones towards cell membrane. Notice that the positive electrically charged MT end corresponds to biologically less dynamically active minus end and vice versa. This biologically positive end is exposed to more intensive growing during MT polymerization Fig. 2.b).

In the following we will present just two aspects of multifunctionality of MTs which manifest in important cellular activities.

First one regards the nonlinear mechanoelectrical excitations in MTs which utilize the energy released by the hydrolysis of GTP (guanosin triphosphate) nucleotide embedded in every tubulin dimer contained in MT matrix.

The second model considers the MTs as true polyelectrolites which enable the formation of condensed ionic clouds around them. The model of nonlinear transmission line explains how MTs can serve as biological electric nanowires capable of conducting cellular signals and efficiently distributing divalent cations (Ca^{2+}, Mg^{2+}) throughout the cell to the places where the need for them does appear [4, 5].

2. *The mechanoelectrical model of microtubule dynamics*

The essential ingredients of MTs relevant for the model considered here are so called tubulin tails (TTs). Each tubulin monomer in the MT lattice has an extended C-terminal alpha-helix H_{12} followed by highly acidic amino acid sequence projecting out of the MT outer surface which is referred to as carboxy-terminal tail, or tubulin tail [6,7].

Geometrically these TTs are hair-like projections of $4 - 5\,nm$ length, depending on the effective charge present, see Fig. 3.

TTs have a high proportion of negatively charged residues, for example a TT of β-tubulin has $9\,Glu$ residues and $2\,Asp$ residues. This needs an adequate number of positive counterions for charge compensation in cellular cytosol. The fluctuation of TT domains are for sure associated with accompanying currents of positive counterions. This aspect will be the subject of the next section.

The circumstance that TTs are negatively charged but these charges are partially compensated by positive counterions, enables that besides the dipole moment of tubulin body an additional dipole moment associated with pertaining TT should be taken into account. This is the reason why the set of TTs within a MT can be considered as a cylindrical layer of ferroelectric

smectic-C liquid crystal folded into a cylinder so that TTs are pointing radially outwards (see Fig. 4).

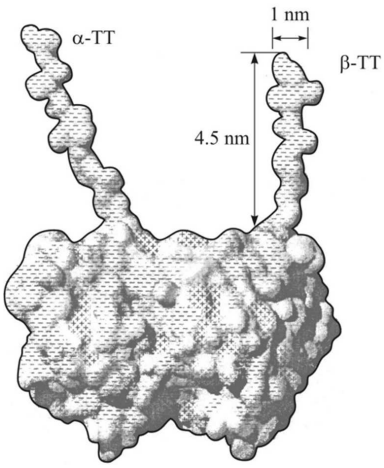

Fig. 3. The landscape of a tubulin dimer with TTs whose dimensions are: the length of 4.5 nm and diameter of 1 nm. The surface charge distribution is indicated by plus and minus signs

Every isolated tubulin heterodimer body has its own dipole moment which is constant and oriented along its longest axis (longitudinally). And every TT has its own dipole moment which is superimposed with dipole of heterodimer's body.

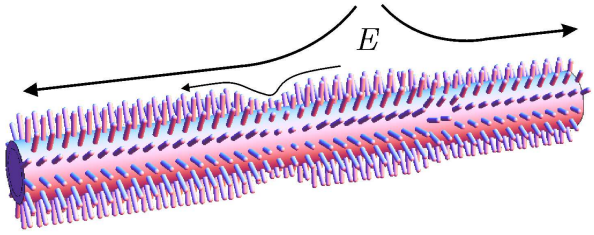

Fig. 4. The sketch of a collection of tubulin tails within a microtubule. The localized name is indicated with accompanying electric field

When a TT tilts about its fixed base its dipole also swings causing that the total dipole moment of a heterodimer with TTs has dynamical character.

The total dipole moment $\vec{p}$ can be expressed as the sum of its longitudinal and transversal components

$$\vec{p} = \vec{p}_\ell + \vec{p}_t; \quad p_\ell = p\sin\gamma; \quad p_t = p\cos\gamma, \tag{2.1}$$

with the illustration in Fig. 5 (left).

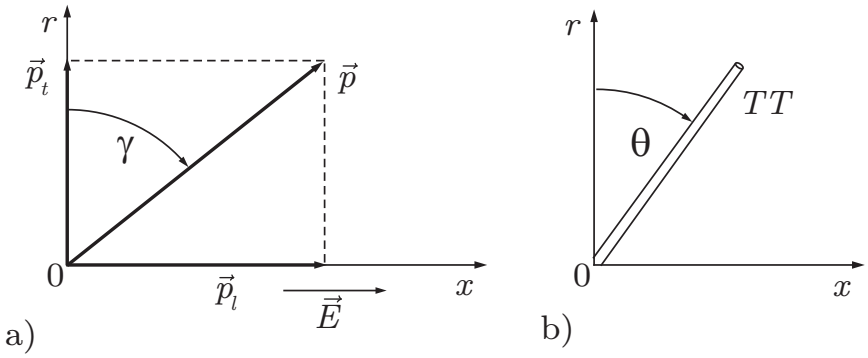

Fig. 5. a) The geometry of a total dipole moment of tubular dimer; b) The polar angle θ for a given TT

We have in mind that along a MT the intrinsic electric field $\vec{E}$ exists in parallel with x axis.

Let take that a TT is tilted for polar angle θ, Fig. 5 (right). Then the density of polarization energy of a MT can be written as follows

$$W_{\text{pol}}\left[\frac{J}{m^3}\right] = \frac{P_\ell^2}{2\chi_\ell} + \frac{P_t^2}{2\chi_t} - EP_\ell - \mu_p P_t \sin\theta. \tag{2.2}$$

Here the polarization is denoted with capital letter $P\,[Db/m^3]$. The corresponding longitudinal and transversal dielectric susceptibilities for MT are denoted by χ_ℓ and χ_t with units (F/m); μ_p is the phenomenological constant, which will be elaborated later.

When a TT is tilted for an angle θ so is $\vec{P}_t$ and its projection on the x-axis can be expressed as $P_t \sin\theta$.

According to the seminal approach by Carlsson, Stewart and Leslie [8, 9], the cylindrical smectic-C liquid crystal thin layer has the elastic energy in cylindrical coordinates as follows

$$W_{layer} = \frac{1}{2r^2}[A_{12}(\theta)\sin^4\varphi + A_{21}(\theta)\cos^4\varphi - 2A_{11}(\theta)\sin^2\varphi\cos^2\varphi], \tag{2.3}$$

where r, θ and φ are radial, polar and azimuthal degree of freedom.

The elastic coefficients $A_{ij}(\theta)$ are even functions of polar angle θ. In original papers [8, 9] the expansion was of quadratic order due to relatively

small θ. In this model since θ can be of the order of radian, we will expand it up to fourth order of θ, as follows

$$\left.\begin{aligned} A_{12}(\theta) &= K_{11} + L_{12}\theta^2 + M_{12}\theta^4, \\ A_{21}(\theta) &= K_{11} + L_{21}\theta^2 + M_{21}\theta^4, \\ A_{11}(\theta) &= -K_{11} + L_{11}\theta^2 + M_{11}\theta^4. \end{aligned}\right\} \tag{2.4}$$

Inserting the expansions Eq. (2.4) in Eq. (2.3) we get

$$\begin{aligned} W_{\text{layer}} = \frac{K_1}{2r^2} &+ \frac{1}{2r^2}[(L_{12}+L_{11})\sin^4\varphi + (L_{21}+L_{11})\cos^4\varphi - L_{11}]\theta^2 \\ &+ \frac{1}{2r^2}[(M_{12}+M_{11})\sin^4\varphi + (M_{21}+M_{11})\cos^4\varphi - M_{11}]\theta^4. \end{aligned} \tag{2.5}$$

Looking for the stable configuration, regarding the azimuthal angle φ, we should minimize the layer energy, Eq. (2.5) with respect to φ,

$$\frac{\partial W_{\text{layer}}}{\partial \varphi} = 0;$$

thus giving

$$(L_{12}+L_{11})\sin^2\varphi - (L_{11}+L_{21})\cos^2\varphi + [(M_{11}+M_{12})\sin^2\varphi - (M_{11}+M_{21})\cos^2\varphi]\theta^2 = 0,$$

or in slightly rearranged form,

$$(L_{12}+L_{11}) + (M_{21}+M_{11})\theta^2]\sin^2\varphi = [(L_{11}+L_{21}) + (M_{11}+M_{21})\theta^2]\cos^2\varphi = 0. \tag{2.6}$$

The expressions in square brackets must have the same sign, so it is plausible to take them with positive signs

$$\left.\begin{aligned} (L_{12}+L_{11}) + (M_{11}+M_{12})\theta^2 > 0, \\ (L_{21}+L_{11}) + (M_{11}+M_{21})\theta^2 > 0. \end{aligned}\right\} \tag{2.7}$$

Thus the stable azimuthal angle is being defined by the expression

$$\varphi_0 = \arctan\left[\frac{(L_{11}+L_{21}) + (M_{11}+M_{21})\theta^2}{(L_{11}+L_{12}) + (M_{11}+M_{12})\theta^2}\right]. \tag{2.8}$$

If the symmetry conditions $L_{12} = L_{21}$ and $M_{12} = M_{21}$ hold, one obtains

$$\varphi_0 = \frac{\phi}{4}. \tag{2.9}$$

Solving for $\sin^2\varphi$ and $\cos^2\varphi$ from Eq. (2.6), and inserting in Eq. (2.5) it follows

$$W_{layer} = \frac{K_{11}}{2r^2} + \frac{1}{2r^2}\left[U\theta^2 + V\theta^4\right], \tag{2.10}$$

where

$$U = (L_{11}+L_{12})\frac{(L_{11}+L_{12})^2}{(L_{12}+L_{21}+2L_{11})^2} + (L_{12}+L_{11})\frac{(M_{11}+M_{12})^2}{(M_{12}+M_{21}+2M_{11})^2} - L_{11}$$

and

$$V = (M_{11}+M_{12})\frac{(L_{11}+L_{12})^2}{(L_{12}+L_{21}+2L_{11})^2} + (M_{11}+M_{12})\frac{(M_{11}+M_{12})^2}{(M_{12}+M_{21}+2M_{11})^2} - M_{11}.$$

Expecting that symmetry conditions leading to Eq. (2.9) safely hold, the simplified version of Eq. (2.5) now reads

$$\left.\begin{aligned} &W_{\text{layer}} = \frac{K_{11}}{2r^2} + \frac{1}{4r^2}(A\theta^2 + B\theta^4), \\ &A = L_{12} - L_{11};\ B = M_{12} - M_{11}, \\ &A < 0;\ B > 0. \end{aligned}\right\} \tag{2.11}$$

The next step is to introduce the energy density of torsional splay along the length of MT in parallel with x-axis,

$$W_{\text{sp}} = \frac{K_{11}}{2}\left(\frac{\partial\theta}{\partial x}\right)^2, \tag{2.12}$$

and the density of rotational kinetic energy

$$W_{\text{kin}} = \frac{1}{2}\mathcal{J}\left(\frac{\partial\theta}{\partial t}\right)^2, \tag{2.13}$$

where $\mathcal{J}$ stands for the density of rotational inertia of TTs when rotate around their fixed ends joined with MT body.

Eventually on the basis of the large tilt angle and appropriate expansion of $\sin\theta$, the density of polarization energy, Eq. (2.2) now reads

$$W_{\text{pol}} = \frac{P_\ell^2}{2\chi_\ell} + \frac{P_t^2}{2\chi_t} - EP_\ell - \mu_p P_t\theta + \frac{1}{6}\mu_p P_t\theta^3. \tag{2.14}$$

If we use the Eq. (2.1) this expression involves the angle γ between tilted polarization vector $\vec{P}$ and the radial axis, thus giving

$$W_{\rm pol} = \frac{P^2 \sin^2\gamma}{2\chi_\ell} + \frac{P^2\cos^2\gamma}{2\chi_t} - EP\sin\gamma \\ -(\mu_p P\cos\gamma)\theta + \frac{1}{6}(\mu_p P\cos\gamma)\theta^3. \qquad (2.15)$$

The polarization energy density, Eq. (2.15) can be minimized with respect to polarization P thus enabling the elimination of P in terms of θ

$$\frac{\partial W_{\rm pol}}{\partial P} = 0, \qquad (2.16)$$

which leads to the expression:

$$\left.\begin{aligned} P &= [E\sin\gamma + (\mu_p\cos\gamma)\theta - \tfrac{1}{6}(\mu_p\cos\gamma)\theta^3]\Lambda(\gamma), \\ \Lambda(\gamma) &= \left[\frac{\cos^2\gamma}{\chi_t} + \frac{\sin^2\gamma}{\chi_\ell}\right]^{-1}. \end{aligned}\right\} \qquad (2.17)$$

Inserting P from Eq. (2.17) into (2.15), we finally get

$$W_{\rm pol} = \Lambda\left[\left(\frac{1}{4}\mu_p^2\cos^2\gamma\right)\theta^4 + \left(\frac{1}{12}E\mu_p\sin(2\gamma)\right)\theta^3 \right. \\ \left. - \left(\frac{1}{2}\mu_p^2\cos^2\gamma\right)\theta^2 - \left(\frac{1}{2}E\mu_p\sin(2\gamma)\right)\theta - \frac{1}{2}E^2\sin^2\gamma\right]. \qquad (2.18)$$

This is the complete polynomial of fourth power with respect to the angle θ.

Even in the case where the electric field E is absent the remaining two terms with even powers assure the existence of double-well potential alike the expression, Eq. (2.11) for layer elastic energy.

We now gather together all the elastic and polarization terms with kinetic energy, Eqs. (2.11), (2.12), (2.13) and (2.18) and thus create the total free energy for the complete collection of TTs within a given MT,

$$F = 2\pi\int_{\mathcal{R}}^{\mathcal{R}+\lambda} r dr \int_{x_1}^{x_2} dx \left[\frac{K_{11}}{2}\left(\frac{\partial\theta}{\partial x}\right)^2 + \frac{\mathcal{J}}{2}\left(\frac{\partial\theta}{\partial t}\right)^2 + \frac{K_{11}}{2r^2} + \frac{1}{4r^2}(A\theta^2 + B\theta^4)\right. \\ + \left(\frac{1}{4}\Lambda\mu_p^2\cos^2\gamma\right)\theta^4 + \left(\frac{1}{12}\Lambda E\mu_p\sin 2\gamma\right)\theta^3 - \left(\frac{1}{2}\Lambda\mu_p^2\cos^2\gamma\right)\theta^2 \\ \left. - \left(\frac{1}{2}\Lambda E\mu_p\sin 2\gamma\right)\theta - \left(\frac{1}{2}\Lambda E^2\sin^2\gamma\right)\right]. \qquad (2.19)$$

Here $\mathcal{R} = 12.5\,nm$ stands for outer radius of a MT and $\lambda = \ell_{eff} = 4.5\,nm$ for the length of a TT indicating the bounds for radial integral. Performing the respective radial integration the last expression yields

$$\begin{aligned} F = \int_{x_1}^{x_2} dx \Bigg\{ & \pi(2\mathcal{R}\lambda + \ell^2) \left[\frac{K_{11}}{2} \left(\frac{\partial\theta}{\partial x} \right)^2 + \frac{\mathcal{J}}{2} \left(\frac{\partial\theta}{\partial t} \right)^2 \right] + \pi K_{11} \ln\left(1 + \frac{\lambda}{\mathcal{R}}\right) \\ & + \frac{\pi}{2} \ln\left(1 + \frac{\lambda}{\mathcal{R}}\right) (A\theta^2 + B\theta^4) + \left[\frac{\pi}{4}(2\mathcal{R}\lambda + \lambda^2)\Lambda\mu_p^2 \cos^2\gamma \right] \theta^4 \\ & + \left[\frac{\pi}{12}(2\mathcal{R}\lambda + \lambda^2)\Lambda E\mu_p \sin(2\gamma) \right] \theta^3 - \left[\frac{\pi}{2}(2\mathcal{R}\lambda + \lambda^2)\Lambda\mu_p^2 \cos^2\gamma \right] \theta^2 \\ & - \left[\frac{\pi}{2}(2\mathcal{R}\lambda + \lambda^2)\Lambda E\mu_p \sin(2\gamma) \right] \theta - \left[\frac{\pi}{2}(2\mathcal{R}\lambda + \lambda^2)\Lambda E^2 \sin^2\gamma \right] \Bigg\} \end{aligned} \tag{2.19}$$

There are two terms expressing the direct coupling of mechanical movement θ with electric field E.

Eventually by minimizing the free energy F from Eq. (2.20) with respect to θ, and equating that result to a viscous damping term

$$F_{\text{vis}} = -\Gamma \frac{\partial\theta}{\partial t} \tag{2.21}$$

we arrive to the Euler-Lagrange equation for polar tilt angle θ

$$\frac{\partial^2\theta}{\partial x^2} - \frac{\mathcal{J}}{K_{11}} \left(\frac{\partial^2\theta}{\partial t^2} \right) - \delta \frac{\partial\theta}{\partial t} - a\theta^3 - b\theta^2 + c\theta + d = 0, \tag{2.22}$$

where the set of pertaining abbreviations read

$$\left.\begin{aligned} \delta = \frac{\Gamma}{\pi K_{11}(2\mathcal{R}\lambda + \lambda^2)}; \quad a = \frac{1}{K_{11}} \left[\frac{2\ln\left(1 + \frac{\lambda}{\mathcal{R}}\right)}{(2\mathcal{R}\lambda + \lambda^2)} B + \Lambda\mu_p^2 \cos^2\gamma \right]; \\ b = \frac{1}{4K_{11}} \Lambda E \sin(2\gamma); \quad c = \frac{1}{K_{11}} \left[\Lambda\mu_p^2 \cos^2\gamma - \frac{2\ln\left(1 + \frac{\lambda}{\mathcal{R}}\right)}{(2\mathcal{R}\lambda + \lambda^2)} A \right]; \\ d = \frac{1}{2K_{11}} \Lambda E\mu_p \sin(2\gamma). \end{aligned}\right\} \tag{2.23}$$

This is nonlinear partial differential equation of motion with an asymmetric double well potential of the following form

$$\prod(\theta) = \frac{1}{4}a\theta^4 + \frac{1}{3}b\theta^3 - \frac{1}{2}c\theta^2 - d\theta. \tag{2.24}$$

If the standard procedure for traveling wave solution of Eq. (2.22) with unified coordinate ξ defined by

$$\xi = \frac{x - vt}{\ell}, \tag{2.25}$$

where v stands for wave velocity and ℓ for a dimer length, is readily performed, then this equation is converted in the nonlinear ordinary differential equation.

The most important outcome is the appearance of the solution which represents the so called kink waves

$$\theta(\xi) = \left(\frac{c}{a}\right)^{1/2} \left(\frac{2}{1 + \exp(\sqrt{2}\xi)} - 1 + \frac{\varepsilon}{\sqrt{27}}\right), \tag{2.26}$$

with

$$\varepsilon = \frac{\sigma B + 1}{1 - \sigma A}; \quad \sigma = \frac{2 \ln\left(1 + \dfrac{\lambda}{\mathcal{R}}\right)}{\Lambda \mu_p^2 \cos^2 \gamma (2\mathcal{R}\lambda + \lambda^2)}. \tag{2.27}$$

This excitations moves with constant velocity preserving the very stable shape, see Fig. 6.

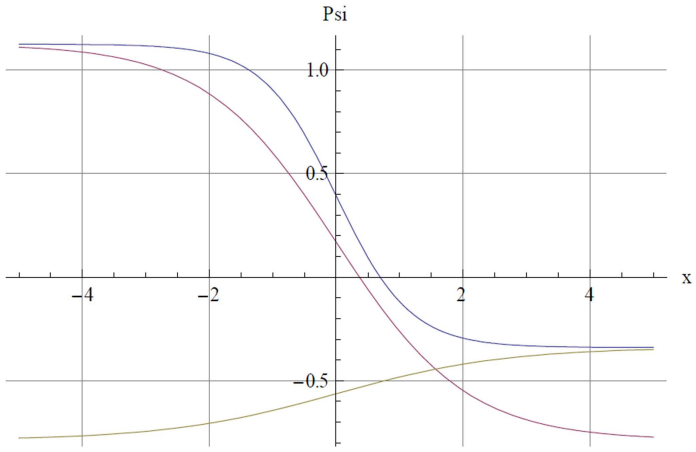

Fig. 6. Two kinks with different initial parameters

The reason for kink stability in despite of the presence of viscous dissipation is the energy supply provided by the action of electric field E.

The constant kink velocity is given by the following expression

$$v = \frac{3v_0}{b}\left(\frac{\mathcal{J}a\lambda}{\ell}\right)^{1/2} q_{\text{eff}}\left(\frac{E}{\Gamma}\right), \tag{2.28}$$

where

$$v_0 = \left(\frac{K_{11}}{\mathcal{J}}\right)^{1/2}$$

is the respective sound velocity while q_{eff} is the effective charge of a dipole associated with single tubulin dimer.

The above result is physically very plausible and is a kind of equivalence with Ohm's law. The velocity is linearly proportional to the strength of electric field and inversely proportional to the viscous damping.

In conclusion, our model leads to the efficient mechanism of lunching and tuning TT kinks along MTs by the control role of intrinsic cellular electric fields. We conjecture that these kinks should play the role of signals which initiate the onset of intracellular traffic and transport of different organelles by motor proteins walking along MTs. The other possible role is related for fast drift of cations, primarily Ca^{2+} and Mg^{2+} implicated in catalyzing of many vital cellular functions. This segment is the subject of the next section.

3. *Nonlinear ionic currents along microtubules*

Extensive molecular dynamics simulations of tubulin dimer structure [3] indicate the existence of a highly negatively charged outer surface of tubulin dimer with a net electric charge on the order of $(20-25)\,e$ per monomer ($e = 1.6 \cdot 10^{-19}\,C$), depending on the isotype of tubulin.

Thus we conclude that MTs are highly charged polyelectrolytes which attract a fraction of their surrounding counter-ions in the form of condensed ionic cloud (IC) preferentially localized around the MT surface.

In the addition negative ions of the cytosol are repelled away from the MT surface and a roughly cylindrical depletion layer around MT and TTs emerges. The thickness of such a depleted area is approximately equal to the so called Bjerrum length denoted by ℓ_B and defined by equating the energy of thermal fluctuations with Coulomb attraction (repulsion) energy between ion species,

$$\frac{ze^2}{4\pi\varepsilon_0\varepsilon\ell_B} = k_BT; \quad \varepsilon_0 = 8.85 \cdot 10^{-12}\,F/m. \tag{3.1}$$

At a physiological temperature ($T = 310\,K$), taking the elementary charge as $e = 1.6 \cdot 10^{-19}\,C$, Boltzman's constant as $k_B = 1.38 \cdot 10^{-23}\,J/K$, and the relative dielectric permittivity of the cytosol as $\varepsilon = 80$, and for Ca^{2+} ions $z = 2$, one readily obtains

$$\ell_B = 1.34 \cdot 10^{-9}\,m = 1.34\,nm. \tag{3.2}$$

Counter-ion condensation occurs when the mean distance between two charges ρ is such that the following inequality

$$S = \frac{\ell_B}{\rho} \gg 1 \tag{3.3}$$

holds. It was estimated that there are some $15-18$ exposed negative charges per tubulin dimer [10]. Since each dimer is $8nm$ long and 13 protofilaments form a MT, one could readily find that there is a linear charge density of $(20-30)(e/nm)$ indicating that linear charge spacing is $\rho = (0.33-0.44) \cdot 10^{-10}m$, safely providing that the condition (3.3) holds,

$$16 < S < 21. \tag{3.4}$$

The second important characterization of a polyelectrolite is the Debye length defined as

$$\ell_{Db} = (8\pi\ell_B n_0)^{-1/2}, \tag{3.5}$$

where n_0 stands for total concentration of ions present in cytosol. The estimated value amounts

$$\ell_{Db} \simeq 2nm. \tag{3.6}$$

This should be greater or comparable with the radius r of concrete rodlike polyelectrolyte considered

$$\ell_{Db} \geq r. \tag{3.7}$$

Since the radius of a TT is of the order of $r_{\mathrm{TT}} = 0.5\,nm$ and the radius of a TD is of the order of $r_{\mathrm{TD}} = 2.5\,nm$ we see that the condition Eq. (3.7) could be met for either.

We are now in the position to establish the model of nonlinear electric transmission line considering a MT as the cable of 13 parallel filaments. Each filament is composed of serie of identical electric elementary units (EEU) represented by single tubulin dimers. Every unit possesses resistive and capacitive properties which should be properly estimated. The condensed ionic cloud and repelled anions play the roles of "conductive plates"

of a cylindrical capacitor while depleted layer plays the role of a dielectric medium [5].

The important point is to estimate the capacitance of a single EEU. It consists of the part pertaining to outer half cylinder of tubulin dimer body plus the part originating from two pertaining TTs. On the basis of cylindrical symmetry the first part contributes as follows (see Fig. 7.a),

$$C_{\mathrm{TD}} = \frac{\pi\varepsilon_0\varepsilon\ell}{\ln\left(1+\dfrac{\ell_B}{r_{ic}}\right)}. \tag{3.8}$$

Starting from the parameters $\ell = 8\,nm$; $\varepsilon = 80$, $\ell_B = 1.34\,nm$ then the outer radius of ionic cloud is $r_{\mathrm{ic}} = r_{\mathrm{TD}} + \lambda_{\mathrm{TD}} = (2.5 + 2.5)\,nm$ and λ_{TD} is the thickness of condensed ionic cloud around tubulin dimer body. Inserting above values in Eq. (3.8) one obtains

$$C_{\mathrm{TD}} = 0.77 \cdot 10^{-16}\,F. \tag{3.9}$$

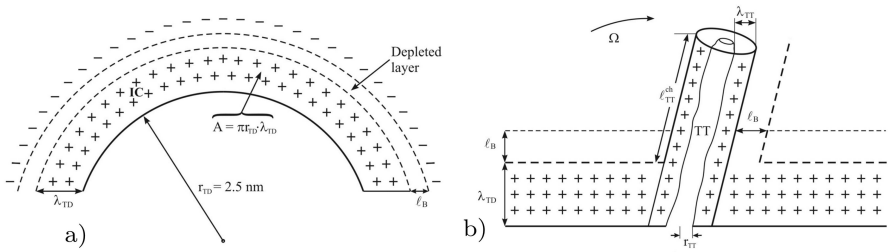

Fig. 7. a) The shape of condensed ionic cloud arround dimer outer surface; b) The ionic condensed cloud arround tubulin tail

Analogously we can consider an extended TT as a smaller cylinder with the radius $r_{\mathrm{TT}} = 0.5\,nm$ and the thickness of its IC is equal to $\lambda_{\mathrm{TT}} = 1\,nm$. Its extended effective length should be $\ell_{\mathrm{TT}}^{\mathrm{eff}} = (4.5 - 2.5)\,nm = 2\,nm$ on the basis of the fact that its part close to the tubulin surface is already embedded in the IC of thickness $\lambda_{\mathrm{TD}} = 2.5\,nm$.

If these parameters were substituted in Eq. (3.8) it follows

$$C_{\mathrm{TT}} = 0.15 \cdot 10^{-16}\,F. \tag{3.10}$$

Accounting for the fact that two TTs are at the same tubulin dimer, the total maximal capacitance of an EEU reads

$$C_0 = C_{\mathrm{TD}} + 2C_{\mathrm{TT}} = 1.07 \cdot 10^{-16}\,F. \tag{3.11}$$

We here emphasize that TT's capacitance must change with an increasing concentration of condensed cations due to the shrinking of flexible TTs. These changes are slightly different due to the different structures of α and β-type TTs. To include this case we introduce the reduced factor of nonlinearity as follows

$$b_0 = \frac{b_\alpha b_\beta}{b_\alpha + b_\beta}, \tag{3.12}$$

where b_α and b_β stand for the respective TTs.

This implies that the change of an EEU capacitor diminishes with an increased voltage in a nonlinear way $\Delta C_0 = C_0 b_0 v;\ \ b_0 v \ll 1$.

Now very importantly we can account the tilting movements of TTs in the context of Section 2. In this case the tilt $\theta(t)$ can appear under the combined action of thermal fluctuations and a locally changing voltage due to an incoming ionic influx.

Thus, the part of EEU capacitance contributed by TTs should also change by TTs tilt as illustrated in Fig. 7.b.

The change of the effective length $\ell_{\rm TT}^{\rm eff}$ of a TT is an additional factor influencing the capacitance $\Delta C_{\rm TT}$. It is reasonable that this change could be described by the small oscillations of TTs,

$$\Delta \ell_{\rm TT}^{\rm eff} = \ell_{\rm TT}^{\rm eff} \sin[\Omega(t - t_0)] \simeq \ell_{\rm TT}^{\rm eff} \Omega (t - t_0), \tag{3.13}$$

where the frequency Ω is much smaller than the inverse charging time of the complete EEU capacitor due to the strong viscous damping of the TT tilt. This fact justifies the above linearization of pertaining sine function in Eq. (3.13).

Including the both aspects of TTs dynamics described above, the charge of an EEU can be expressed by the following nonlinear function of local voltage

$$Q = C_0 \Big[1 - \Gamma_0 \Omega (t - t_0) - b_0 v \Big] v, \tag{3.14}$$

where Γ_0 is a dimensionless parameter.

The second important electrical parameter of EEU is the Ohmic resistance.

The dominant ionic flow is in parallel with the MT axis charging EEU capacitors. The leaking through the depleted layer could be ignored but there is some leaking into the MT lumen through two different nanopores which are open between neighboring tubulin dimers of nearest protofilaments, see Fig. 8.

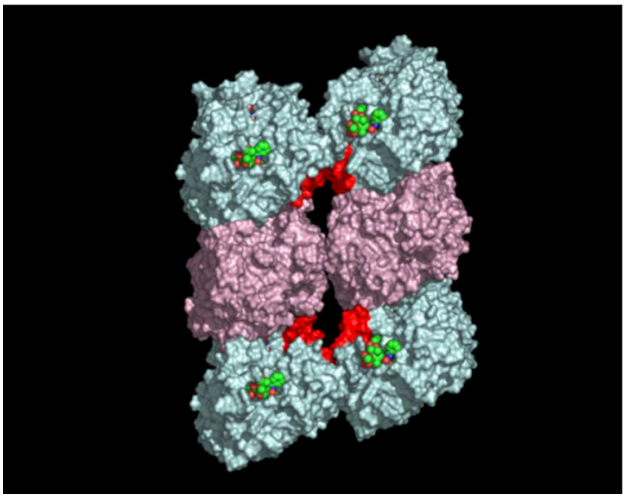

Fig. 8. The nanopores within a microtubule

The in silico experiments performed by H. Freedman et al [11] yield the resistance for complete 13 protofilaments $R_{\rm MT} = 4.75 \cdot 10^6 \Omega$. The resistance for our EEU should be 13 times greater giving

$$R_0 = 6.2 \cdot 10^7\, \Omega. \tag{3.15}$$

In the same reference [11] the conductance of both leaking nanopores was estimated to be

$$G_0 = G_1 + G_2 = (2.93 + 7.8)\, nS = 10.7\, nS; \quad \frac{1}{G_0} = R_{\rm NP} = 9.3 \cdot 10^7\, \Omega. \tag{3.16}$$

It is now possible to construct the periodically repeating long ladder network composed of a lumped section equal to EEU consisting of the elements given by Eqs. (3.14), (3.15), (3.16), see Fig. 9.

By applying the Kirchoff's law governing currents and voltages, from Fig. 9 we obtain

$$\left.\begin{aligned} i_n - i_{n+1} &= \frac{\partial Q_n}{\partial t} + G_0 v_n, \\ v_{n-1} - v_n &= R_0 i_n. \end{aligned}\right\} \tag{3.17}$$

Taking the time derivative of Eq. (3.14) and inserting in Eq. (3.17) we

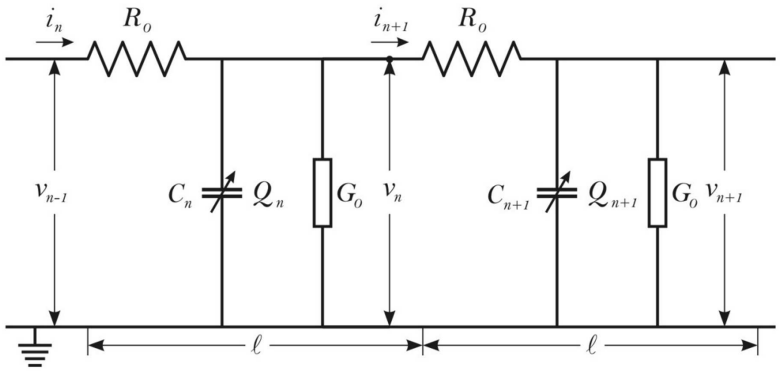

Fig. 9. An effective circuit diagram for the n-th ER with characteristic elements for Kirchhoff's laws

arrive at the system of nonlinear difference–differential equations as follows

$$\left.\begin{aligned} i_n - i_{n+1} &= C_0\frac{\partial v_n}{\partial t} - C_0\Gamma_0\Omega v_n - C_0\Gamma_0\Omega(t-t_0)\frac{\partial v_n}{\partial t} \\ &\quad -2b_0C_0v_n\frac{\partial v_n}{\partial t} + G_0v_n, \\ v_{n-1} - v_n &= R_0i_n. \end{aligned}\right\} \tag{3.18}$$

Bearing in mind that the discrete voltage v_n, as well as the current i_n, change gradually from an EEU to its neighbors we can implement the standard expansion of $v_n \pm 1$ and $i_n \pm 1$ in a continuum approximation using Taylor's series with respect to a small distance parameter ℓ ($\ell = 8\,nm$ is the length of an EEU). In parallel we can go over to the unifying auxiliary function $u(x,t)$ defined by

$$u(x,t) = Z^{1/2}i(x,t) = Z^{-1/2}v(x,t), \tag{3.19}$$

where the characteristic reactive impedance of an EEU is expressed in the usual way as

$$Z = \frac{1}{C_0\omega}. \tag{3.20}$$

In the next step we use the traveling-wave form of the function $u(x,t)$,

$$u(x,t) = u(\zeta - \tau); \quad \zeta = \frac{x}{\ell}; \quad \tau = s\frac{t}{T_0}; \quad s = \frac{v}{v_0} \leq 1, \tag{3.21}$$

with new dimensionless arguments (ξ, τ). Here the characteristic time T_0 of charging of an EEU capacitor C_0 through the resistance R_0 has the following value

$$\left.\begin{aligned} T_0 &= R_0 C_0 = 6.2 \cdot 10^7 \Omega \times 1.07 \cdot 10^{-16} F = 6.6 \cdot 10^{-9} s, \\ \omega &= \frac{2\pi}{T_0} = \frac{6.28}{6.6} \cdot 10^9 s^{-1} = 9.5 \cdot 10^8 s^{-1}. \end{aligned}\right\} \tag{3.22}$$

The characteristic velocity of the ionic drift is defined as follows

$$v_0 = \frac{\ell}{T_0} = \frac{8 \cdot 10^{-9} m}{6.6 \cdot 10^{-9} s} = 1.2 \left(\frac{m}{s}\right). \tag{3.23}$$

After a straightforward evaluation we eventually get the following inhomogeneous nonlinear partial differential equation

$$\left(\frac{ZC_0 s}{T_0} - 2\right) \frac{\partial u}{\partial \tau} + \frac{1}{3} \frac{\partial^3 u}{\partial \zeta^3} + ZC_0 \Gamma_0 \Omega (\zeta - \zeta_0) \frac{\partial u}{\partial \zeta}$$

$$+2 \frac{Z^{3/2} b_0 C_0 s}{T_0} u \frac{\partial u}{\partial \zeta} + (ZG_0 + Z^{-1} R_0 - 2C_0 \Gamma_0 \Omega) u = 0. \tag{3.24}$$

After lengthy calculations given in very details in Ref. [5] we readily obtained the most interesting and imporant solution of Eq. (3.24) as follows

$$u(\zeta, \tau) = \frac{u_0 \exp(-2g\tau)}{\cos h^2 \left\{ \left[\frac{hu_0}{4q} \exp(-2g\tau)\right]^{1/2} \left[\delta + \frac{hu_0}{3q} [\exp(-2g\tau) - \exp(9\tau)\right] \right\}}, \tag{3.25}$$

where the abbreviations were introduces as to read

$$\begin{aligned} h &= \frac{2Z^{3/2} b_0 C_0 s}{T_0 \left(\frac{ZC_0 s}{T_0} - 2\right)}, \qquad q = \left[3\left(\frac{ZC_0 s}{T_0} - 2\right)\right]^{-1}, \\ g &= \frac{ZC_0 \Gamma_0 \Omega}{\left(\frac{ZC_0 s}{T_0} - 2\right)}, \qquad \Gamma_0 = \frac{G_0}{3C_0 \omega} + \frac{C_0 R_0 \omega}{3}, \\ \Gamma_0 &= \frac{G_0}{3C_0 \omega} + \frac{C_0 R_0 \omega}{3}, \quad \delta = \zeta - \zeta_0 (1 - \exp(g\tau)), \end{aligned} \tag{3.26}$$

and u_0 is the initial amplitude of either the voltage or the current of ionic condensed cloud.

In order to perform the numerical simulation of Eq. (3.24) we start by estimating the value for the factor which should not be zero in order to avoid the singularity in Eq. (3.24).

On the basis of Eq. (3.20) we first calculate the impedance of an EEU, using Eq. (3.22):

$$Z = \frac{1}{C_0\omega} = \frac{T_0}{C_0 2\pi} = \frac{6.6 \cdot 10^{-9} s}{1.07 \cdot 10^{-16} F \cdot 6.28} = 9.8 \cdot 10^6\,\Omega. \tag{3.27}$$

So, the following estimation holds (for $s = 1$):

$$\left(\frac{ZC_0 s}{T_0} - 2\right) = \frac{9.8 \cdot 10^6 \cdot 1.07 \cdot 10^{-16}}{6.6 \cdot 10^{-9}} - 2 = -1.84, \tag{3.28}$$

and the dimensionless parameter of TTs tilt frequency from Eq. (3.26) gives

$$\Gamma_0 = 2.13. \tag{3.29}$$

In order to estimate the mechanical frequency Ω of tilting TTs we can start from the expression

$$\frac{1}{2}\mathcal{J}_{\mathrm{TT}}\Omega^2 = k_B T \tag{3.30}$$

which leads to the rough estimation

$$\Omega \sim 2 \cdot 10^8\, s^{-1}. \tag{3.31}$$

Comparing Eq. (3.31) with Eq. (3.22) we see that the mechanical frequency is small compared with electrical one so that the approximation in Eq. (3.13) is safely justified.

If we use the set of estimated parameters in Eqs. (3.26), (3.27), (3.28) and (3.29) we are able to apply the MATLAB program and to solve for the function Eq. (3.25) (see Fig. 10).

We obtained the bell-shaped localized solitonic solution. It appears that increased value of nonlinearity parameter h from Eq. (3.26) exhibits not only a higher localization but faster propagation and slower decay of soliton's amplitude. The advantage of this excitation lies in the fact that its speed decreases very slightly on the path of a few micrometers, which is the order of the cell's diameter. This property assures that MTs can be considered as biological electrical wires capable of conducting ionic pulses which are necessary for important cellular function including learning and memory activities of neuron cells.

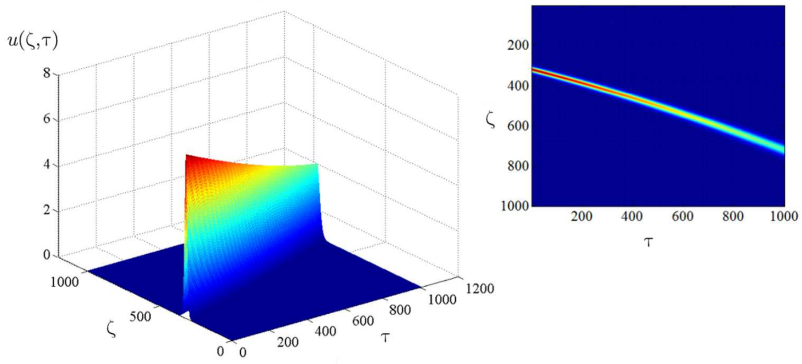

Fig. 10. Numerical solution of $u(\zeta, \tau)$

4. *General conclusion and discussion*

This paper deals with two interesting aspects of nonlinear dynamics of microtubules. First part was dedicated to mechanoelectrical waves excited to propagate in terms of tilting swings of so called tubulin tails the hair like extrusions from tubulin dimers.

These localized waves are so called kink solitons. They are capable to play the role of signals for intracellular signaling and communications. We predict their involuments in regulation of intracellular traffic which is highly organized without traffic jam in healthy cells. Second part deals with microtubules as polyelectrolites. Interestingly in this segment tubulin tails again play the crucial role in providing the nonlinearity which underly of the appearance of localized condensed ionic clouds which propagate along microtubules. This mechanism provides faster and more tunable way of transport of important ions (primarily Ca^{2+} and Mg^{2+}) providing their controlable catalytic actions in many cellular functions.

REFERENCES

[1] P. Dustin, *Microtubules*, Springer, Berlin, 1984.

[2] J. A. Tuszynski, S. Hameroff, M. V. Satarić, B. Tripisova, M. L. Nip, *Ferroelectric behavior in microtubule dipole lattices: implications for information processing, signaling and assembly/disassembly*, J. Theor. Biol. **174** (4) (1995), 371–380.

[3] J. A. Tuszynski, J. A. Brown, E. Crawford, E. J. Carpenter, M. L. A. Nip, J. M. Dixon, M. V. Satarić, *Molecular dynamics simulations of tubulin structure and calculations of electrostatic properties of microtubules*, Math. Comput. Modelling, **41** (2005), 055–1070.

[4] M. V. Satarić, D. Ilić, N. Ralević, J. A. Tuszynski, *A nonlinear model of ionic wave propagation along microtubules*, Eur. Biophys. J. **38** (5) (2009), 637–647.

[5] D. L. Sekulić, B. M. Satarić, J. A. Tuszynski, M. V. Satarić, *Nonlinear ionic pulses along microtubules*, Eur. Phys. J. E. **34** (2011), 49 (11 pages); doi: 10.1140/epje/i2011-11049-0.

[6] E. Nogales, S. G. Wolf, K. H. Downing, *Structure of the $\alpha\beta$ tubulin dimer by electron crystallography*, Nature **391** (1998), 199–203.

[7] M. A. Jimenez, J. A. Evangelio, C. Aranda, A. Lopez-Braunet, D. Andreu, M. Rico, R. Lagos, J. M. Andreu, O. Monasterio, *Helicity of alpha(404–451) and beta(394–445) tubulin C-terminal recombinant peptides*, Protein Science **8** (4) (1999), 788–799.

[8] T. Carlsson, I. W. Stewart, F. M. Leslie, *Theoretical studies of smectic C liquid crystals confined in a wedge. Stability considerations and Frederiks transitions*, Liq. Cryst. **9** (5) (1991), 661–678.

[9] T. Carlsson, I. W. Stewart, F. M. Leslie, *Formation of walls in cylindrical smectic C layers in the presence of a tilted magnetic field*, Liq. Cryst. **11** (1) (1992), 49–61.

[10] N. A. Baker, D. Sept, S. Jospeh, M. J. Holst, J. A. McCammon, *Electrostatics of nanosystems: Application to microtubules and the ribosome*, Proc. Natl. Acad. Sci. U. S. A. **98**, No. 18 (2001), 10037–10041.

Faculty of Technical Sciences
Trg D. Obradovića 6
21000 Novi Sad
Serbia
e-mail: bomisat@neobee.net